

Article

Development of Seawater Intrusion Vulnerability Assessment for Averaged Seasonality of Using Modified GALDIT Method

Il Hwan Kim , Il-Moon Chung  and Sun Woo Chang * 

Department of Land, Water and Environmental Research, Korea Institute of Civil Engineering and Building Technology, Goyang 10223, Korea; kimilhwan@kict.re.kr (I.H.K.); imchung@kict.re.kr (I.-M.C.)

* Correspondence: chang@kict.re.kr; Tel.: +82-31-910-0278

Abstract: Climate change and anthropogenic activities are necessitating accurate diagnoses of seawater intrusion (SWI) to ensure the sustainable utilization of groundwater resources in coastal areas. Here, vulnerability to SWI was assessed by classifying the existing GALDIT into static parameters (groundwater occurrence (G), aquifer hydraulic conductivity (A), and distance from shore (D)) and dynamic parameters (height to groundwater-level above sea-level (L), impact of existing status of seawater intrusion (I), and aquifer thickness (T)). When assessing the vulnerability of SWI based on observational data (2010–2019), 10-year-averaged data of each month is used for GALDIT dynamic parameter for representing the seasonal characteristics of local water cycles. In addition, the parameter L is indicated by the data observed at the sea-level station adjacent to the groundwater level station. The existing GALDIT method has a range of scores that can be divided into quartiles to express the observed values. To sensitively reflect monthly changes in values, the range of scores is divided into deciles. The calculated GALDIT index showed that the most vulnerable month is September, due to relatively low groundwater level. The proposed method can be used to apply countermeasures to vulnerable coastal areas and build water resources management plan considering vulnerable seasons.

Keywords: GALDIT; monthly vulnerability; seawater intrusion (SWI); vulnerability assessment; effective weight; densely populated area



Citation: Kim, I.H.; Chung, I.-M.; Chang, S.W. Development of Seawater Intrusion Vulnerability Assessment for Averaged Seasonality of Using Modified GALDIT Method. *Water* **2021**, *13*, 1820. <https://doi.org/10.3390/w13131820>

Academic Editors: Evangelos Tziritis and Andreas Panagopoulos

Received: 21 May 2021
Accepted: 24 June 2021
Published: 30 June 2021

Publisher's Note: MDPI stays neutral with regard to jurisdictional claims in published maps and institutional affiliations.



Copyright: © 2021 by the authors. Licensee MDPI, Basel, Switzerland. This article is an open access article distributed under the terms and conditions of the Creative Commons Attribution (CC BY) license (<https://creativecommons.org/licenses/by/4.0/>).

1. Introduction

Coastal areas host large populations of people owing to their prosperity. Since the 20th century, 21 megalopolises in the coastal areas have grown rapidly to achieve a population of more than eight million, and more than a third of the global population resides within 100 km of the shore [1]. With the increasing area affected by seawater intrusion (SWI) in coastal areas, the available amount of water resources is decreasing due to the aquifer salinization. Furthermore, changes caused by the salinization of coastal aquifers, such as limitations in the cultivation environment of agricultural and marine products, are damaging economic activities [2,3].

The land-use changes due to industrial development increase surface runoff and decrease recharge of the groundwater system. Furthermore, climate change increases rainfall intensity due to change in the rainfall pattern. As the number of days without rain rises, the amount of water resources discharged to the surface increases, while that of recharge to the aquifer decreases. Consequently, groundwater resources gradually decrease [4–8]. The continuous rise in sea levels accelerates the increase in the SWI range with respect to freshwater body, seawater–freshwater interface and mixing zone [9]. According to the analysis method of Ghyben–Herzberg, the effect of a 1 m rise in the sea level on the freshwater aquifer corresponds to 40 m of freshwater thickness [10–12]. Sherif and Singh [13] claimed that when the sea level rises by 0.5 m, the effect of SWI reaches up to 9 km from the shore. The imbalance between the inflow and outflow from the aquifer can

cause a faster drop in the freshwater groundwater level in areas with a larger pumping water quantity [14]. SWI accelerates due to the extensive use of groundwater in coastal areas, and the resulting effects by the excessive pumping of groundwater are being actively researched [15–21]. To efficiently establish response measures to SWI damage, one must select an area of most active SWI damage and choose response measures in line with the regional characteristics. Research on seawater intrusion in coastal aquifers through the use of monitoring data, assessing groundwater quantity and quality by using modeling, and improving management approaches is being actively conducted [22]. One diagnostic method is the SWI assessment for a coastal groundwater aquifer. The general vulnerability assessment method for groundwater resources involves overlaying thematic maps linked with the scored geographic information system (GIS) data, using the overlaying technique and assessing vulnerability according to the value [23]. For the vulnerability assessment, the range of fixed scores is classified and presented under subjective judgment, depending on the values and types of factors associated with groundwater resources [24,25]. The vulnerability of groundwater resources is defined as their sensitivity to human activities and natural phenomena, and the recharge required to maintain groundwater resources and the possibility of the spread of pollutants by potential pollution sources have likewise been defined [26]. Representative vulnerability parameters for the potential pollution of groundwater resources include DRASTIC ([27]; Depth to groundwater, net Recharge, Aquifer media, Soil media, Topography, Impact of the vadose zone, and hydraulic Conductivity), and SINTACS (depth to the groundwater table (S), effective infiltration (I), unsaturated zone attenuation capacity (N), soil attenuation capacity (T), hydrogeological characteristics of the aquifer (A), hydraulic conductivity (C), and topographical slope (S)) [28]. To consider the effect of coastal aquifers on SWI, GALDIT ([29]; groundwater occurrence (G), aquifer hydraulic conductivity (A), height of groundwater level above the sea (L), distance from the shore (D), impact of the existing status of SWI (I), and saturated thickness of the aquifer (T)) was developed as a representative vulnerability assessment method. GALDIT is highly reliable in assessing seawater intrusion vulnerability in coastal aquifers [30]. Recently, the assessment method of the GALDIT index has been modified for the range of the existing score and weight [31,32]. The parameter replacement of GALDIT factors and the improvement of data interpolation methods have been researched, as well [33–35].

Several previous studies on SWI in South Korea addressed the inflow of seawater into the aquifer, using the seawater monitoring network (SIMN) that was built at the national level [36]. Numerous studies on SWI have also been conducted on Jeju Island in South Korea [37]. A vulnerability assessment for SWI, using GALDIT for Jeju Island, was conducted for the first time in South Korea [38]. Recently, studies on seawater intrusion in the inland areas of Korea are incomplete compared with those in the island areas, but studies on the coastal areas of the west coast have started. For example, Kim and Yang [39] prioritized three SWI response measures for SWI-vulnerable areas when climate change was applied using the multi-criteria decision-making (MCDM) method. Chun et al. [40] conducted a two-dimensional numerical analysis of the effects of SWI on coastal areas according to different climate change scenarios.

Studies on SWI can set different time scales according to the study objectives. For example, studies on the mid-to-long-term effects of SWI, such as climate change, use time scales of ten to several hundred years [16,18–20]. In contrast, studies on short repetitive variation characteristics, such as tidal effects, conduct hourly analyses use small time scales [41–43]. In the past, techniques such as vulnerability assessments used representative values obtained through statistical tests of longer-term data [44,45]. To establish response measures to SWI, the flow characteristics according to the periods of saltwater and freshwater groundwater resources must also be considered. The assessment of flow characteristics for groundwater resources consists of factors for the spatial distribution and temporal changes in the groundwater level recorded in a time series [46,47].

Therefore, the objective of this study was to develop a method to assess SWI vulnerability for averaged seasonality based on the original GLADIT. GALDIT is the most

representative SWI assessment method, and the reliability of the method is guaranteed through continuous research. Modified GALDIT methods have been applied to regions with various hydrogeological properties. In this study, the modified GALDIT method for assessing the averaged seasonality is used to intuitively and easily express monthly data with various fluctuations.

Data on SWI of coastal aquifers over the last 10 years were collected to analyze the monthly variations. The monthly vulnerability changes of the SWI were analyzed by classifying the collected data into monthly means. The GALDIT method, which is the most representative SWI assessment method, was used. We attempted to indicate spatiotemporally vulnerable areas and periods by classifying the six parameters of GALDIT into parameters that change monthly (L, I, and T) and parameters that change little over time (G, A, and D).

2. Materials and Methods

2.1. Data Collection for Monthly GALDIT Assessment

GALDIT is a diagnostic method based on the index and ranking that evaluates the vulnerability of coastal aquifers, using six parameters, considering groundwater occurrence (G), aquifer hydraulic conductivity (A), distance from the shore (D), height of groundwater level above sea level (L), impact of the existing status of seawater intrusion (I), and saturated thickness of the aquifer (T) to examine the physical effects of coastal aquifers on the SWI. We developed a monthly assessment method for seawater intrusion vulnerability, using GALDIT parameters. Data were collected from the National Groundwater Information Center [48], the National Geographic Information Institute [49], and the Korea Hydrographic and Oceanographic Agency [50]. The groundwater level, drill log, and groundwater survey report data were collected from the National Groundwater Information Center. Digital elevation maps (DEM) and topographic map data were collected from the National Geographic Information Institute. Tidal and other data were collected from the Korea Hydrographic and Oceanographic Agency.

For a monthly vulnerability assessment of the SWI, the parameters that were relatively static and those that changed temporally were classified as (i) static parameters and (ii) dynamic parameters, respectively. For the static parameter group, G, A, and D were selected. The aquifer type and A are regarded relatively static parameters in the absence of human activities. D changes when the sea level rises in the long term; however, this was excluded in this study considering that the monthly change of the coastline due to the sea level is insignificant compared to the reference value. With regard to D, the data observed to date were used without considering the future rises in the sea level. Fluctuations in D were extracted from the average distances obtained in the last 10 years.

For the input data of the parameters that change with time, we employed L, I, and T. The data collected for dynamic parameters included groundwater level, seawater level, and electrical conductivity, and the average data for 10 years per month were extracted. As shown in Figure 1, monthly data for sea level and precipitation data around the groundwater level station are collected. As an example, observation data from 2010 to 2019 were used at Gimpo Walgot groundwater level station, Ganghwa Bridge seawater level station, and Gimpo precipitation station. Observed data were averaged for 10 years each month. The groundwater and seawater level stations are located in the Gimpo area, north of the study area. The Ganghwa Bridge seawater level station is located about 3.2 km away from the Gimpo Walgot groundwater level station. The groundwater level is on average 6.59 m above the reference sea level for the last 10 years. The highest was 6.77 m in July, and the lowest was 6.51 m in March. The electrical conductivity showed an average of 370.71 s/cm over the last 10 years, the highest at 387.55 s/cm in December and lowest at 359.53 s/cm in June. The sea level is located 3.32 m above the reference sea level for the last 10 years, highest being 3.58 m in August and lowest being 3.14 m in January. When showing the distribution of dynamic parameters around Gimpo Walgot, L is the most vulnerable at 2.97 m in August, where the difference between the groundwater level and

seawater level is the smallest. Parameter I appear to be the most vulnerable in December, where the electrical conductivity is the highest, and T is the most vulnerable in July, where the groundwater level is highest. The seasonality of the dynamic parameter appears differently depending on the complex characteristics of the observed area. The parameter L was calculated using the difference between the groundwater and seawater level data observed based on the reference sea level. Each groundwater level station was compared with the sea level data of the nearest seawater level station. In I, data collection is possible and the continuously observed electrical conductivity is used; I is described in detail in Section 3.2.2. T was calculated through the drilling log of the groundwater level station. T was calculated by estimating the height of the aquifer bottom of the drilling log. Through the observed L, I, and T data, the data from the station were used as point source data and spatially interpolated to evaluate GALDIT. Figure 2 shows a flowchart for calculating monthly GALDIT parameters.

2.2. Modification of Original GALDIT Method

GALDIT is a model employed for assessing the vulnerability of underground aquifers to seawater intrusion using six parameters related to seawater intrusion. Data about these six parameters were collected and scored according to the criteria, and maps for the parameters were generated by applying predefined weights. Scores of 2.5, 5, 7.5, and 10 were determined according to the criteria. A weight of four was assigned to the index having the greatest effect on seawater intrusion, and the weight varied by the effect. The relationship between the index according to the criteria and weight of the index is expressed as follows:

$$GALDIT = \frac{\sum_{i=1}^6 (W_i \times R_i)}{\sum_{i=1}^6 W_i} \tag{1}$$

where W_i is parameter i 's weights, and R_i is parameter i 's importance rating.

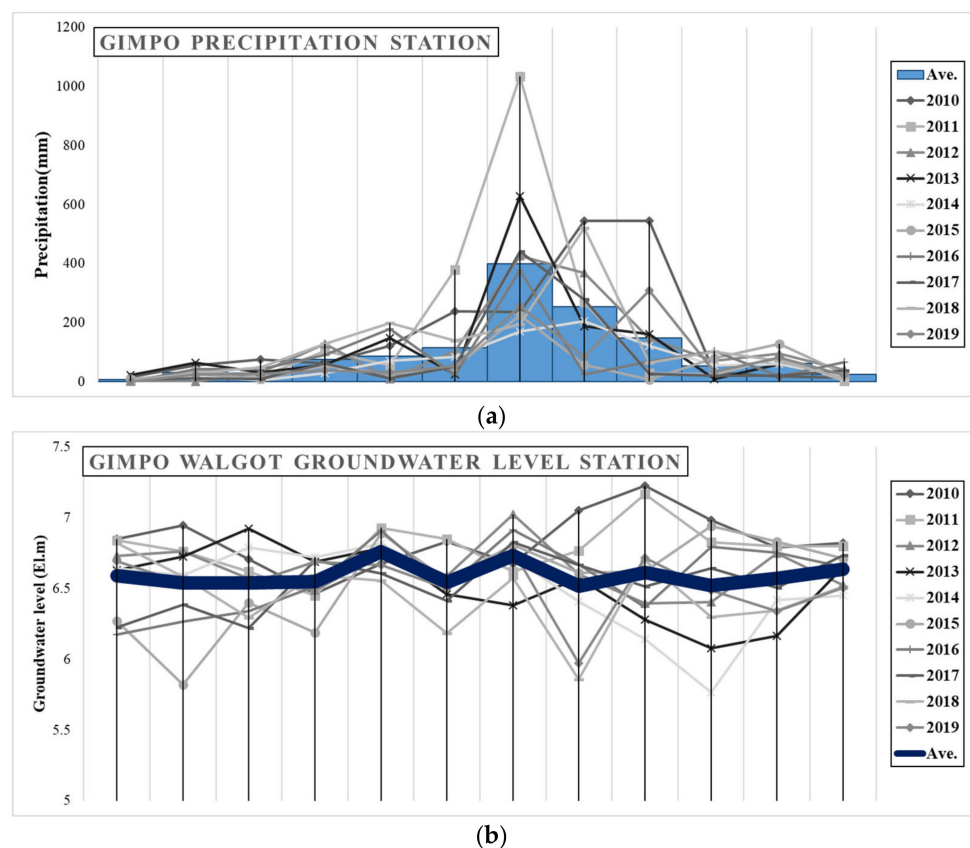


Figure 1. Cont.

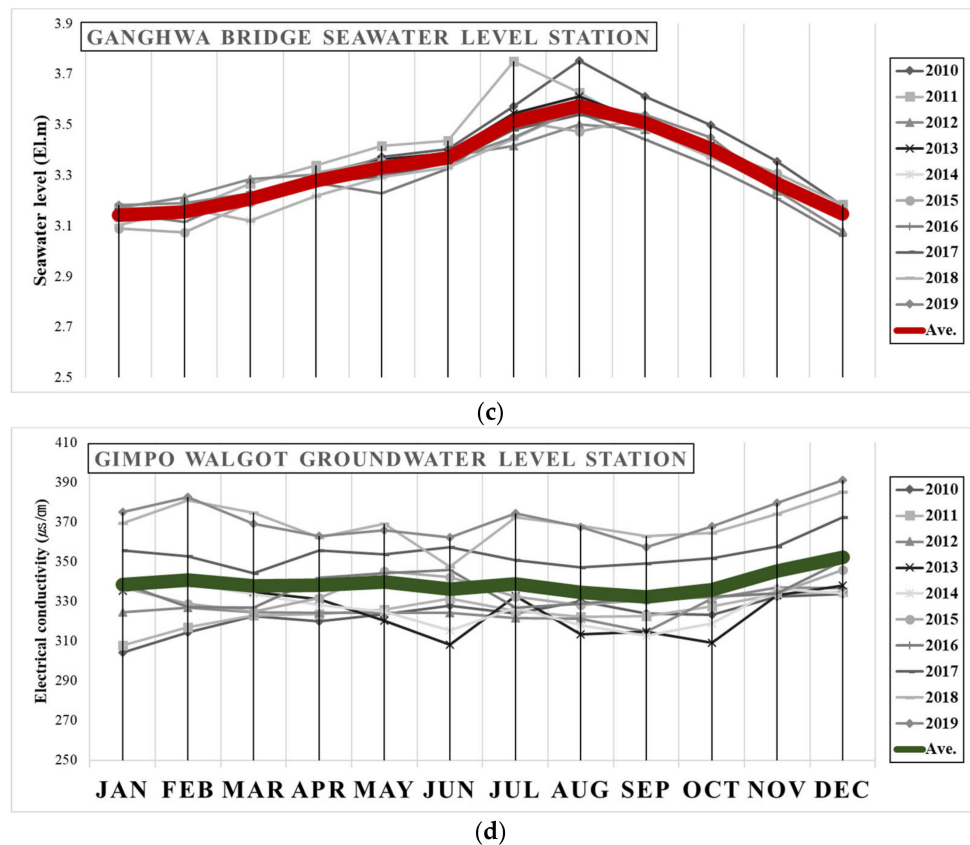


Figure 1. Example of 10-year-averaged monthly (a) precipitation, (b) groundwater level, (c) seawater level, and (d) electrical conductivity observation data.

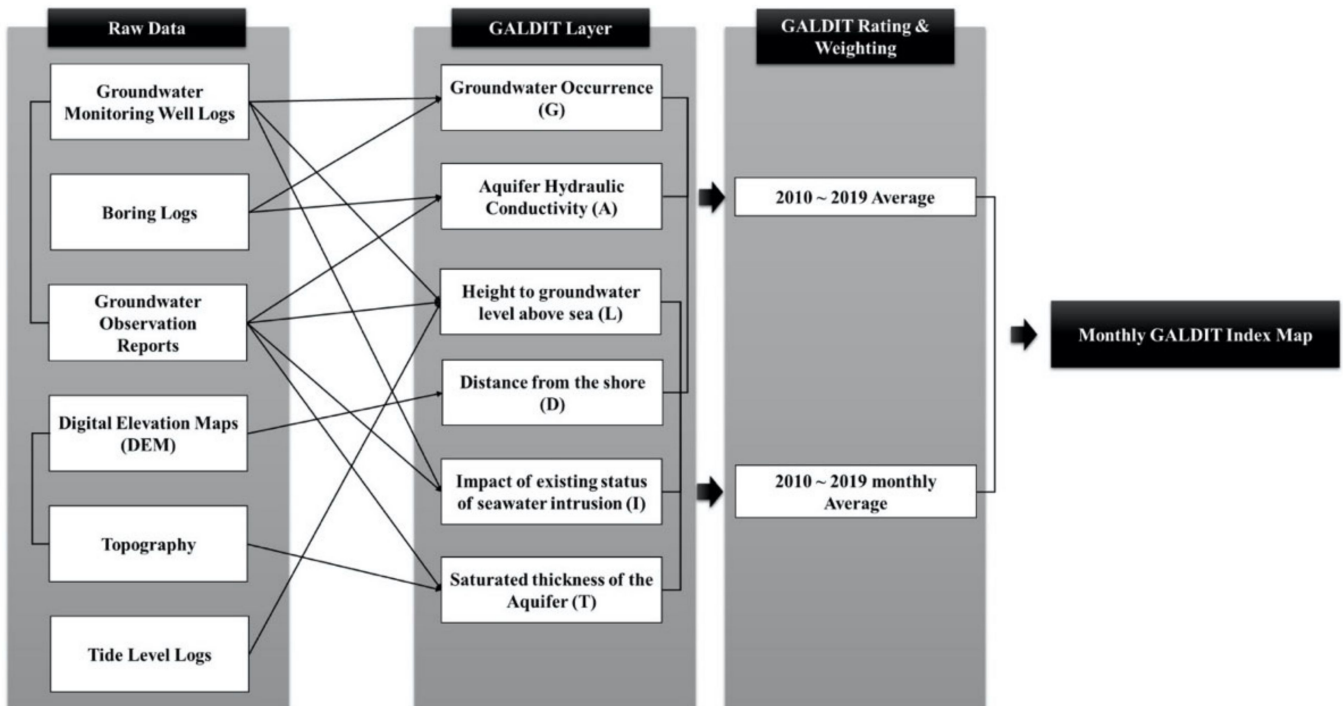


Figure 2. Procedure of monthly-based GALDIT index assessment.

Table 1 lists the ratings and weights according to the criteria for each parameter. According to the scoring method of the existing GALDIT, the highest score was 10, whereas the lowest was 2.5. The highest score was divided using the quartile method into 10, 7.5, 5, and 2.5, according to the parameter range. In this study, the GALDIT factor variable range and the importance rating in the two columns were modified in the right column of Table 1. Thus, the highest score of 10 was divided by using the decile method, and a score between 1 and 10 was assigned for the modified importance rating. The existing quartile method was used to classify aquifers according to their hydrogeological characteristics. The new distributions of scores for other parameters are listed in Table 2.

Table 1. Theoretical weights and rates for GALDIT.

Parameter	Weight	GALDIT Factor Variable Range	Importance Rating
Groundwater occurrence	1	Confined aquifer	10
		Unconfined aquifer	7.5
		Leaky confined aquifer	5
		Bounded aquifer	2.5
Aquifer hydraulic conductivity (m/day)	3	>40	10
		10–40	7.5
		5–10	5
		<5	2.5
Height of groundwater level above sea level (m)	4	<1.0	10
		1.0–1.5	7.5
		1.5–2.0	5
		>2.0	2.5
Distance from shore (m)	4	<500	10
		500–700	7.5
		750–1000	5
		>1000	2.5
Impact of existing status of seawater intrusion ($\mu\text{s}/\text{m}$)	1	>3000	10
		2000–3000	7.5
		1000–2000	5
		<1000	2.5
Saturated thickness of aquifer (m)	2	>10	10
		7.5–10	7.5
		5–7.5	5
		<5	2.5

Table 2. Modified rates for GALDIT.

Parameter	Modified Variable Range	Modified Importance Rating
Groundwater occurrence	Confined aquifer	10
	Unconfined aquifer	7.5
	Leaky confined aquifer	5
	Bounded aquifer	2.5
Aquifer hydraulic conductivity (m/day)	>40	10
	34–40	9
	28–34	8
	22–28	7
	16–22	6
	10–16	5
	8–10	4
	6–8	3
	4–6	2
	<4	1

Table 2. Cont.

Parameter	Modified Variable Range	Modified Importance Rating
Height of groundwater level above sea level (m)	<1.0	10
	1.0–1.2	9
	1.2–1.4	8
	1.4–1.6	7
	1.6–1.8	6
	1.8–2.0	5
	2.0–2.2	4
	2.2–2.4	3
	2.4–2.6	2
>2.6	1	
Distance from shore (m)	<500	10
	500–600	9
	600–700	8
	700–800	7
	800–900	6
	900–1000	5
	1000–1100	4
	1100–1200	3
	1200–1300	2
>1300	1	
Impact of existing status of seawater intrusion ($\mu\text{s}/\text{m}$)	>3000	10
	2600–3000	9
	2200–2600	8
	1800–2200	7
	1400–1800	6
	1000–1400	5
	600–1000	4
	200–600	3
	<200	2
-	1	
Saturated thickness of aquifer (m)	>10	10
	9–10	9
	8–9	8
	7–8	7
	6–7	6
	5–6	5
	4–5	4
	3–4	3
	2–3	2
<2	1	

2.3. Study Area

Korea has long coastlines and various coastal terrains, as it is surrounded by sea on three sides. According to recent data, the lengths of the western, southern, and eastern coastlines span approximately 4900, 3300, and 600 km, respectively [51]. The west coast has numerous bays, peninsulas, capes, and islands due to the crooked and broken coastline. In particular, a ria coast is developing in the coastal areas of the Dadohae and Taean Peninsula, where extremely crooked coastlines are present. Furthermore, this is also a place where numerous soils of terrestrial origin are transported and deposited owing to the gentle terrain slope, severe tidal differences, and the flow through of Korea's great rivers. Consequently, large tidal flats develop along the west coast, and low hilly mountains or large and small coastal plains are distributed inland.

Among the sea areas under the influence of seawater intrusion in South Korea, the western coast with severe tidal differences was targeted, where the coastline is long and the terrain slope is gentle. The selected study area was a coastal area of the inland,

excluding islands in the north, where urban areas are concentrated on the western coast of South Korea. The study area consists of nine administrative districts: Incheon, Asan, Ansan, Gimpo, Hwaseong, Siheung, Pyeongtaek, Dangjin, and Osan. In all of these nine areas, the manufacturing industry is developing, and urbanization is accelerating, leading to a continuous influx of population. Incheon is the third most-populated city in South Korea after Seoul and Busan and has a developed logistics industry, as it hosts the Incheon International Airport and Incheon Port. Ansan is a planned industrial city, where a population of a similar size to the residential one flows during the day due to numerous manufacturing plants. The manufacturing industry is also developed in Gimpo, Hwaseong, Siheung, Pyeongtaek, Dangjin, and Osan. There is Sihwa Lake Seawall in Siheung, Hwaseong, and Ansan, where industrial clusters and tourist attractions are developed. Daebu Island, the only island in the study area, was included in the study area because it is connected to a freshwater lake through the Sihwa Lake Seawall. The total area of the study is 3976.59 km², and the length of the coastline is 608.1 km. The automatic monitoring data and drill logs of the National Groundwater Information Center were used to assess the seawater intrusion vulnerability of the study area. There were 58 groundwater level stations in total. Further, seawater levels were observed at nine seawater level stations. Figure 3 shows the locations of the study area, rivers, coastlines, groundwater level stations, and sea water level stations.

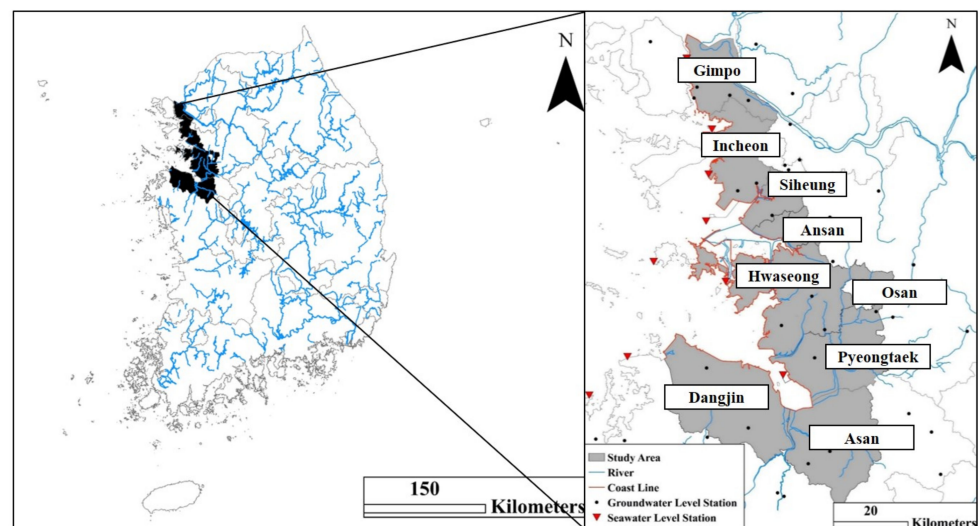


Figure 3. Study area in the western coastal region of South Korea.

3. Results

3.1. Static GALDIT Parameters

In this section, we examine the analysis results for parameters with slight changes over time, i.e., groundwater occurrence (G), aquifer hydraulic conductivity (A), and distance from the shore (D). The histogram colors in Figure 4 represent the ratings divided by the decile method, and the values were divided into 11 levels by adding 7.5 of the unconfined included in G. The *y*-axis represents the cumulative ratio of the area according to the rating, the secondary *y*-axis represents the index score, and the values indicated by the broken line represent the total average of the study area.

Groundwater occurrence (G) is caused by confined, unconfined, leaky, and bounded aquifers, out of which the confined aquifer is the most vulnerable. The scores of groundwater occurrence were divided into four levels, in the same way as the existing scoring method, using a theoretical weight of one. We assessed the alluvial layer in a free-surface aquifer of a shallow area. The aquifer type in all areas was an unconfined aquifer, and the G score was 7.5. Figure 5a shows the G index.

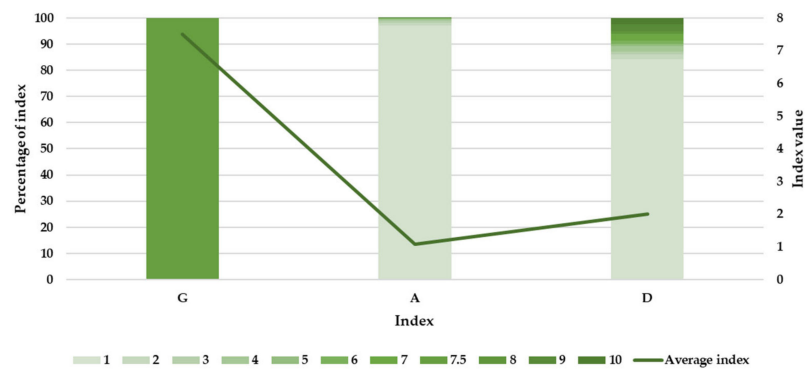


Figure 4. Distribution of static parameters’ ratings for groundwater occurrence (G), aquifer hydraulic conductivity (A), and distance from the shore (D).

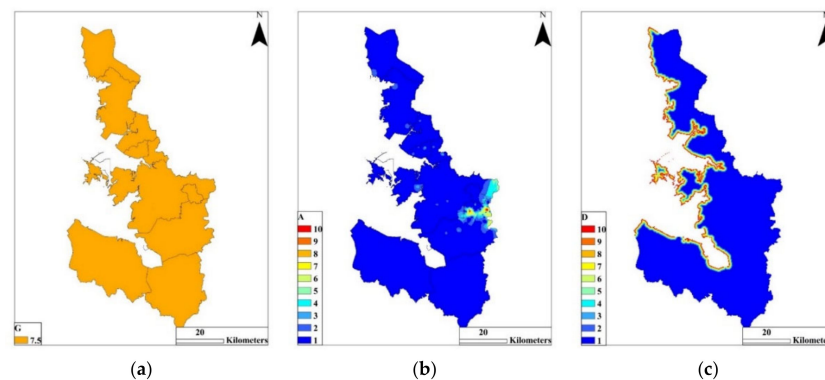


Figure 5. Thematic maps of static parameters’ rating for (a) groundwater occurrence, G, (b) aquifer hydraulic conductivity, A, and (c) distance from shore, D.

A higher A induces smoother groundwater flow and exhibits larger vulnerability to the SWI. The theoretical weight was three in this case. When the aquifer hydraulic conductivity exceeds 40 m/day, it is the most vulnerable, and a score of 10 is attributed to it. When the aquifer hydraulic conductivity was less than 4 m/day, a score of one was given. Examination of the area ratios of each score yields A below 4 m/day at the largest ratio of 94.23%. Some areas have a high aquifer hydraulic conductivity near Pyeongtaek. The total average score of the study area was determined as 1.07. Figure 5b shows the distribution of A.

D was determined based on the observed coastline. Areas below 500 m away from the shore are most vulnerable to SWI, and those more than 1300 m from the coast are given a score of one. The theoretical weight, an index that can intuitively show vulnerability, was four. Most parts of the study area, accounting for 84.14%, were 1300 m from the shore. Areas 1000 m or less away from the shore with a score of less than five accounted for 10.88%, and those less than 500 m away accounted for 2.46%. The average score of the study area was 1.86. Figure 4 shows the percentages and average scores of the static GALDIT parameters. Figure 5c shows the distribution of the D index.

3.2. Dynamic GALDIT Parameters

3.2.1. Height of Groundwater Level above Sea Level (L)

In this section, we examine the analysis results of monthly averages for the data from 2010 to 2019 regarding the parameters that change significantly over time, that is, the height of the groundwater level above sea level (L), the impact of the existing status of seawater intrusion (I), and saturated thickness of the aquifer (T).

L was most vulnerable to SWI when it was less than 1 m, and the score was 10 in this case. When L exceeds 2.6 m, the score is the lowest at one, and the theoretical weight

is four. This index changes monthly. The existing calculation method is used to observe L and compare the range values. In this study, the score was determined by comparing the measured groundwater level from the sea level, with the monthly sea level height measured at the sea water level station. The sea level observation data of the sea water level station were interpolated by setting the coastline as the domain. Figure 6 shows the dynamic parameter's rating for 10-year-averaged height of groundwater level above sea level for each month. L was determined by the minimum distance to the interpolated coastline. The histogram in Figure 7 shows the distribution of scores represented by the decile method. The y -axis on the left is the cumulative ratio of data L according to the rating, and the secondary y -axis represents the average of the data expressed in a straight line. As a consequence of calculating the monthly groundwater height relative to sea level, April exhibited the highest average of the study area, at 1.25, and August had the lowest average, at 1.21. Owing to the nature of Korea's climate, the groundwater level of the unconfined aquifer rises during the rainy season or when intensive rainfall from June to August occurs. The sea level also rose the most in August; however, the increase in the sea level was smaller than that of the groundwater level, and it was the lowest. The variations in groundwater level differed depending on the area, albeit the sea level was the lowest in January and February. Under low rainfall in April and concentrated use of groundwater, the groundwater level drops significantly, making it a period that is most vulnerable to SWI.

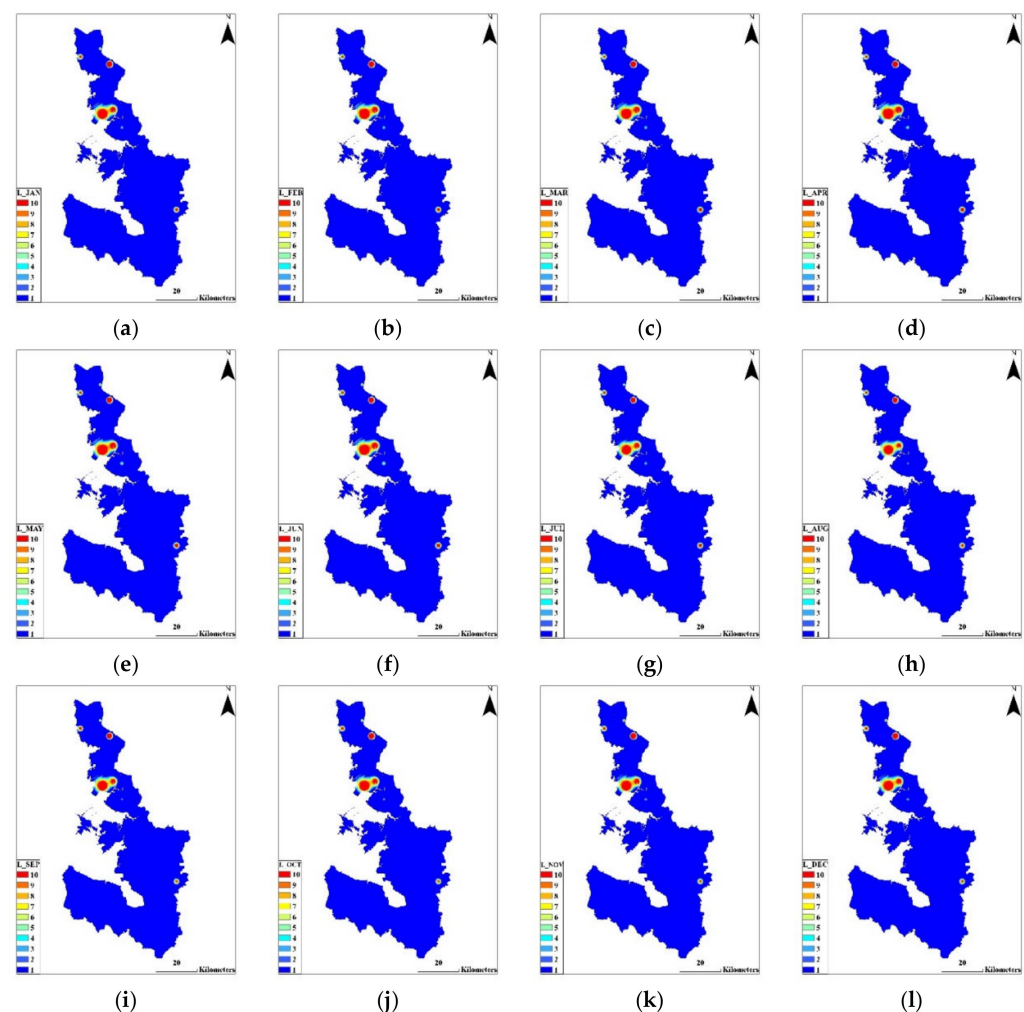


Figure 6. Thematic maps of the dynamic parameter's rating for 10-year-averaged monthly height of groundwater level above sea level (L); (a) JAN; (b) FEB; (c) MAR; (d) APR; (e) MAY; (f) JUN; (g) JUL; (h) AUG; (i) SEP; (j) OCT; (k) NOV; (l) DEC.

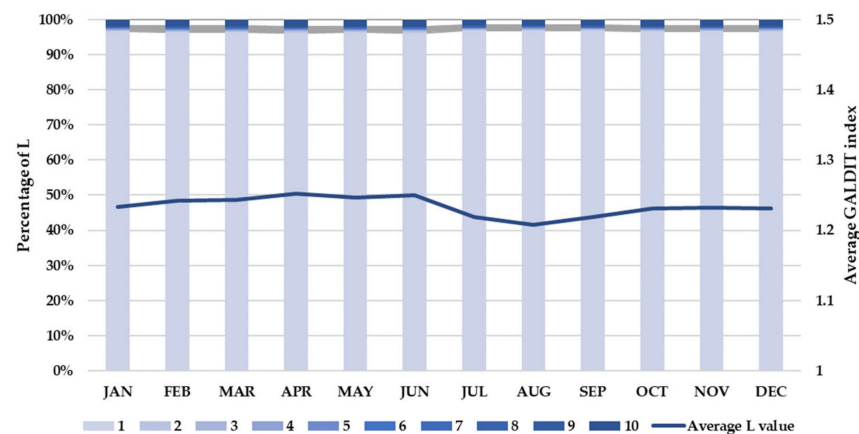


Figure 7. Distribution of the dynamic parameter's rating for 10-year-averaged monthly height of groundwater level above sea level (L).

3.2.2. Impact of the Existing Status of Seawater Intrusion (I)

For the current SWI situation, we used electrical conductivity data, which is easily obtained from national groundwater monitoring network in Korea. Existing studies used the molar ratio of Cl^- ; however, observations were irregular, and the requirement for the length of continuous data could not be satisfied. Chang et al. [38] used the electrical conductivity data obtained from the seawater intrusion monitoring network as input data for the I parameter in the GALDIT assessment. Here, high-quality electrical conductivity data obtained from the National Groundwater Monitoring Network were used. Based on the rating of Chang et al. [38], electrical conductivity above $3000 \mu\text{S}/\text{m}$ led to the highest vulnerability, and a score of two was attributed if it was below $200 \mu\text{S}/\text{m}$. This index can indicate monthly changes, and the theoretical weight of the current SWI situation is one. When the thematic map in Figure 8 is examined with the naked eye, one can observe that the change in parameter values is not large in most areas. However, the area in the north of the study area shows higher values in March, and the values remained high until April and dropped from May. The values increased again in September, slightly decreased in October, and were maintained at 3 to 4 in November. The straight line in the graph in Figure 8 represents the average parameter value for each month. The colors in the histogram in Figure 9 express the rating divided by the decile method. The y -axis on the left is the cumulative ratio of data I according to the rating, and the secondary y -axis on the right represents the average of the data expressed by a straight line. Comparing the monthly average parameters, we see that the most vulnerable month is September, with the average of all areas at 3.65, whereas the least vulnerable month is February, with the average at 3.32.

3.2.3. Saturated Thickness of the Aquifer (T)

T was determined by using drill logs (www.gims.go.kr (accessed on 22 February 2021)). The bottom point of the unconfined aquifer was estimated by analyzing the sample and stratum composition from the drill logs. T was calculated from the height of the groundwater level observed in real time. High-quality data over a continuous period of 10 years were used among the groundwater level data observed in real-time. The saturated thickness of the aquifer is most vulnerable to SWI when it exceeds 10 m, and it is satisfactory when it is less than 2 m, and the score is one. The theoretical weight of T was two.

Figure 10 shows the dynamic parameter's rating for 10-year-averaged saturated thickness of aquifer for each month. The colors in the histogram in Figure 11 express the ratings divided by the decile method. The y -axis represents the cumulative ratio of the area according to the rating, the secondary y -axis represents the scores of the index, and the values indicated by the broken line indicate the total average of the study area. The analysis reveals the minimum score to be four, which indicates all T values were above 4 m. August was the most vulnerable month, at 9.12, and April had the lowest score, at 8.92.

T is an index related to the real-time groundwater level. It is believed that T increases in July and August when significant recharge occurs due to rainfall, and it decreases from February to April when there is fewer rainfall and increased pumping of groundwater.

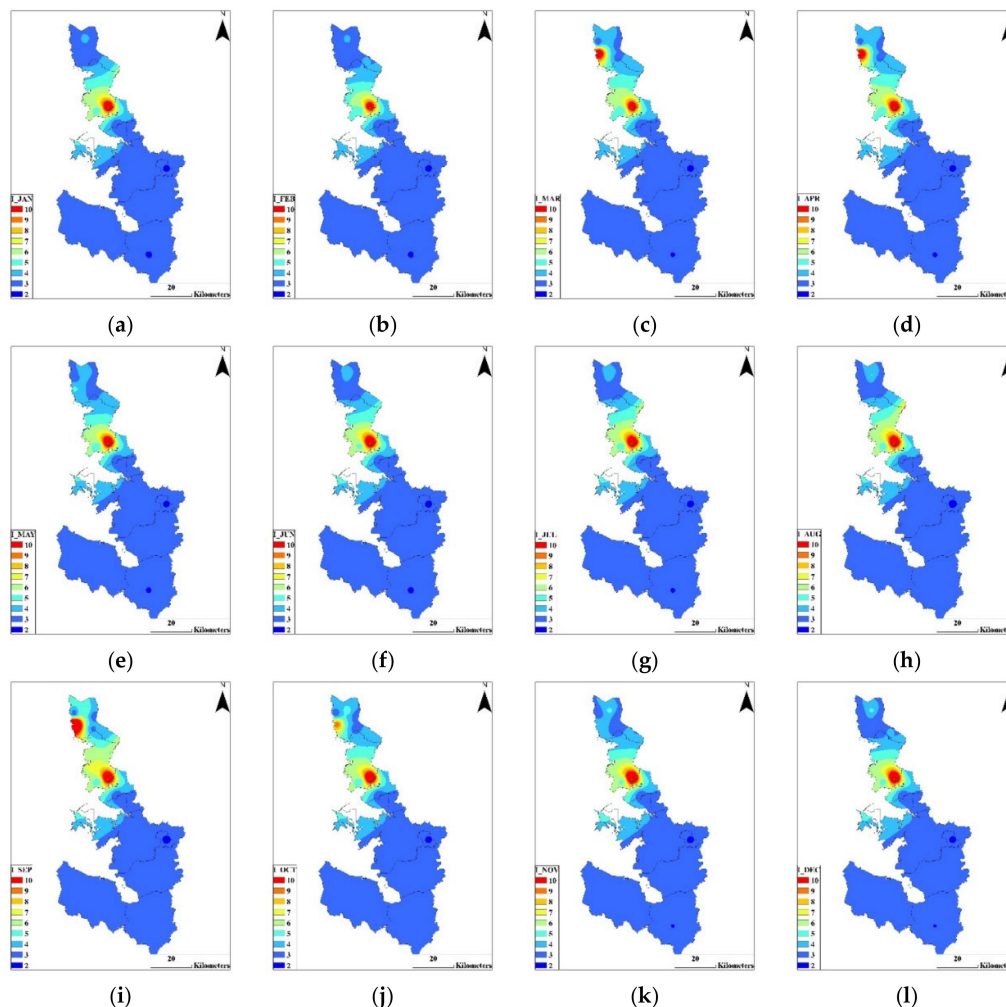


Figure 8. Thematic maps of the dynamic parameter’s rating for 10-year-averaged monthly impact of existing status of seawater intrusion (I). (a) JAN; (b) FEB; (c) MAR; (d) APR;(e) MAY;(f) JUN; (g) JUL; (h) AUG; (i) SEP; (j) OCT; (k) NOV; (l) DEC.

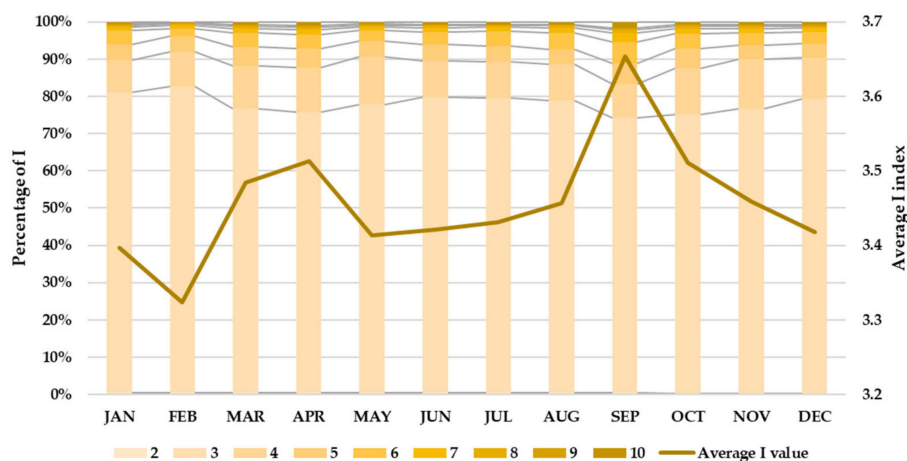


Figure 9. Distribution of the dynamic parameter’s rating for 10-year-averaged monthly impact of existing status of seawater intrusion (I).

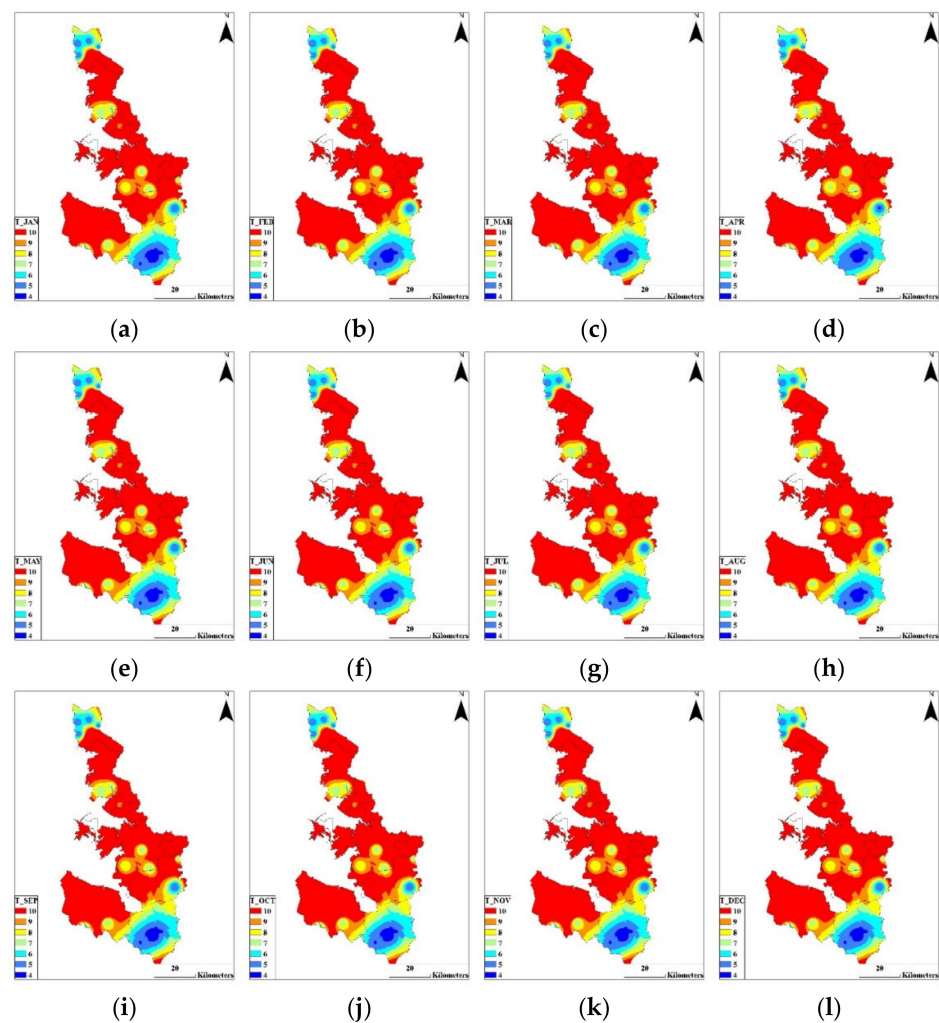


Figure 10. Thematic maps of the dynamic parameter rating for 10-year-averaged monthly saturated thickness of aquifer (T). (a) JAN; (b) FEB; (c) MAR; (d) APR; (e) MAY; (f) JUN; (g) JUL; (h) AUG; (i) SEP; (j) OCT; (k) NOV; (l) DEC.

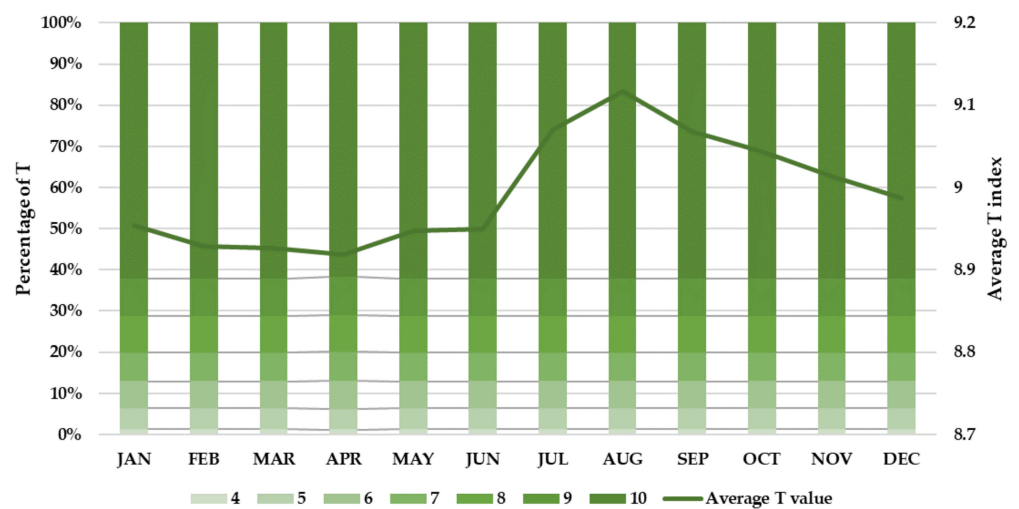


Figure 11. Distribution of the dynamic parameter's rating for saturated thickness of aquifer (T).

3.3. SWI Assessment of Study-Site Based on Monthly GALDIT Index

For the monthly GALDIT index to which the theoretical weight was applied, the average of observations for 10 years was applied for G, A, and D, whereas the parameters that changed monthly were applied for L, I, and T. The colors of the histogram in Figure 12 express the range of the calculated GALDIT index. The y -axis represents the cumulative ratio of the area according to the index range, the secondary y -axis represents the GALDIT index, and the value indicated by the broken line represents the average GALDIT index of the entire study area. The score range that occupied the highest proportion was 2 to 3, which accounted for 78% each in February, May, and July. The calculation results show that the most vulnerable month was September, when the average GALDIT index of the study area was 3.03. The ratio of areas estimated as moderate or high vulnerable with scores ≥ 5 was the highest in September (8.87%), followed by October (8.64%), and April (8.63%). In September, L was relatively robust at 1.19 as the third place from the bottom. However, it was the most vulnerable month in terms of I and the third from the top in terms of T. Thus, it was the most vulnerable month when the theoretical weight was applied. Figure 13a,b shows the original quartile results, and Figure 13c,d shows the decile results. Figure 13a,c shows the result of 10-year-averaged GALDIT maps, and Figure 13b,d shows that of the GALDIT map of September, which is the most vulnerable month as per monthly GALDIT results. In Figure 13a, the coastal area in the south of Incheon and areas near Incheon and Siheung are vulnerable, where the index value is approximately 8 to 9. Upon comparison of the GALDIT map for September in Figure 13d with the original, we see that the index of the Gimpo area indicated in yellow in the northeastern side of the study area is 5 to 6 in most periods, exhibiting a moderate vulnerability. The western coast area of Gimpo, not appearing in the original GALDIT, shows an index value of 7 to 8, indicating the boundary between moderate and high vulnerability. The SWI-vulnerable area on the southern coast of Incheon has an index value of 6 to 7 at both edges around the area protruding to the coast, showing a different pattern from the original GALDIT map. In the Pyeongtaek area, the eastern inland area exhibited low vulnerability. However, in the monthly GALDIT map, the yellow parts showed index values of 3–5, revealing differences in the seawater intrusion vulnerability. Most of the areas excluding the coast showed little differences in the degree; however, in the monthly GALDIT map, they showed partial differences, indicating a low vulnerability. In the entire study area, the inland areas up to 1 km away from the coastline are considered areas of moderate-to-high vulnerability.

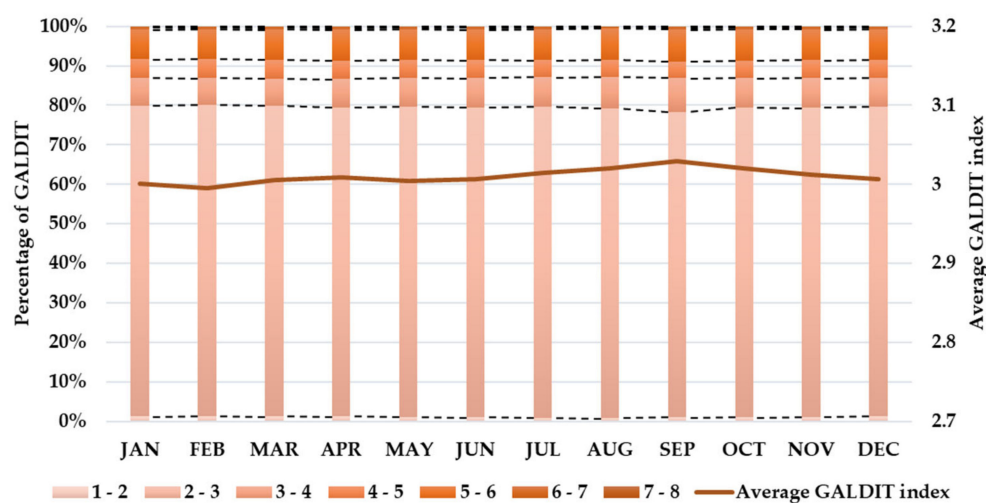


Figure 12. Distribution of 10-year-averaged monthly GALDIT index.

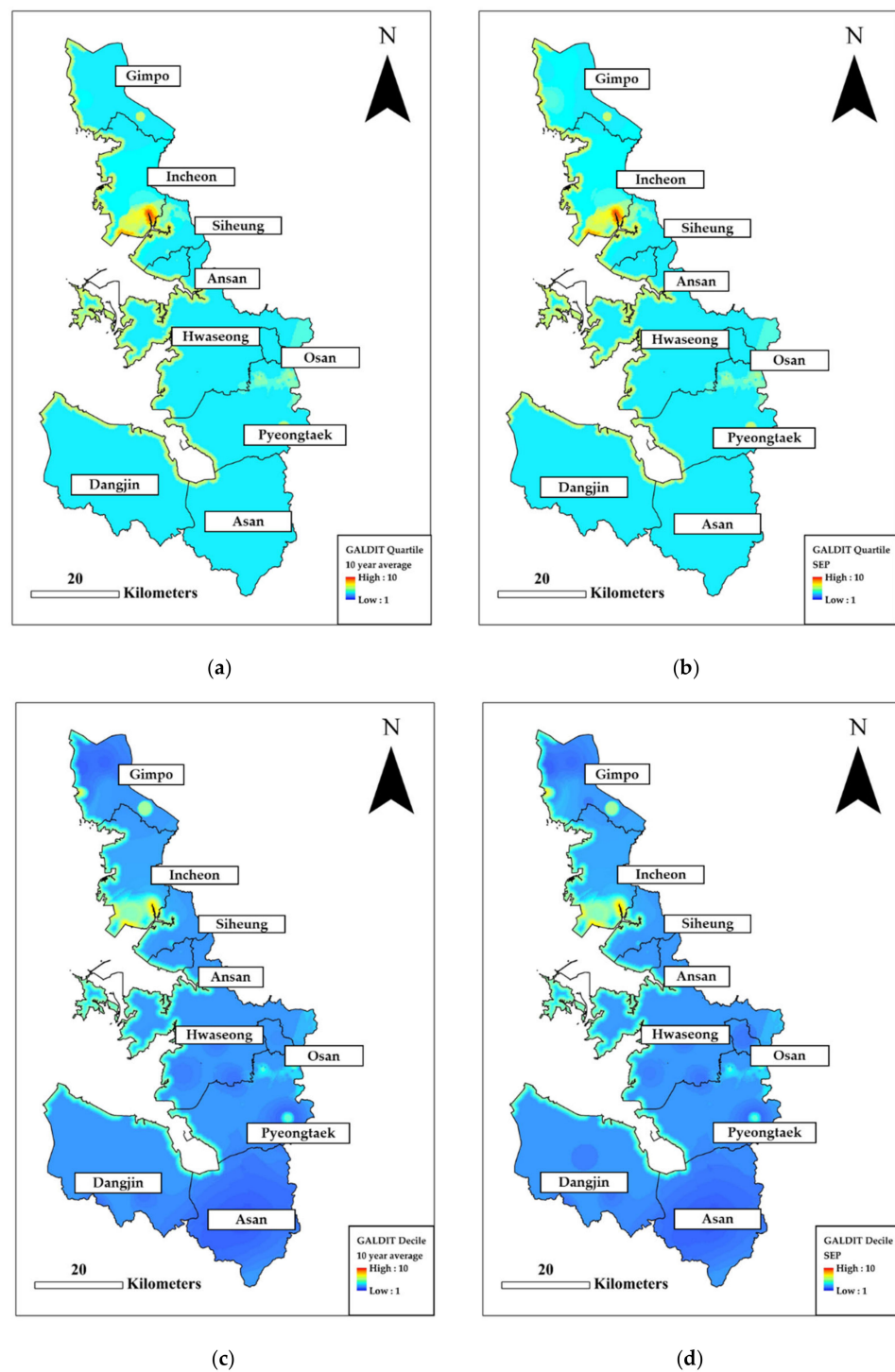


Figure 13. Comparison of (a) 10-year-averaged GALDIT in original quartile classification, (b) GALDIT in September in original quartile classification, (c) 10-year-averaged GALDIT in decile classification, and (d) GALDIT in September in decile classification.

4. Conclusions

SWI into aquifers is accelerating the depletion of coastal groundwater resources. An accurate diagnosis of SWI vulnerability is required for the sustainable utilization of groundwater resources in coastal areas. GALDIT is an SWI vulnerability assessment method that shows representative values, using a statistical test of observed data. The existing assessment method has a wide range of scores to express changing observation values.

To accurately represent regional characteristics or extreme climate patterns, there has been a continuing need for improved vulnerability assessments. Therefore, we developed a method to assess SWI vulnerability for averaged seasonality based on the original GALDIT. The analysis method was differentiated by classifying the six parameters of the existing GALDIT into static and dynamic parameters. For the static parameters—G (groundwater occurrence), A (aquifer hydraulic conductivity), and D (distance from the shore)—similar to the existing method, the annual average or short-term observed values was used. For the dynamic parameters—L (height to groundwater level above sea level), I (impact of existing status of seawater intrusion), and T (thickness of the aquifer)—10-year-averaged monthly data were used to reflect the observed values that change every month. In the existing score range, GALDIT values from the most vulnerable to least vulnerable values are divided by quartiles for the assessment of SWI vulnerability. The values assigned to each parameter were divided by using the decile method to sensitively reflect the degree of vulnerability that changes every month in areas having seasonal variation of the dynamic index, as in South Korea.

As a result of calculating the 10-year-averaged monthly GALDIT index by applying the existing weight, September was determined as the most vulnerable month, having a value of 3.03. In September, the ratio of areas with a score of five or higher was the highest at 8.87%, and it was the most vulnerable month for I and the third most vulnerable month for T. Based on this suggested method, areas that were particularly vulnerable in September, such as Gimpo and Pyeongtaek, were identified on the GALDIT map.

In the 10-year-averaged monthly seawater intrusion assessment, the saturated thickness of the aquifer is somewhat high, and most areas can be easily intruded by seawater. Because of T, which is mostly thick, it is difficult to indicate the differences in vulnerability even if time variability is considered. L was determined based on the sea level observed by sea water level stations near the groundwater level measuring site.

Our SWI vulnerability assessment method can prioritize the most vulnerable places and times according to month. If the countermeasures to the spatially vulnerable areas are prioritized and an operation management schedule is established according to the vulnerable period, the damage from seawater intrusion can be minimized. In addition, establishing a groundwater development and management plan for an area unaffected by SWI is possible.

Recently, various attempts have been made to mitigate and prevent seawater intrusion damage. Mitigation methods for the impact of the existing status of SWI after the occurrence of SWI include installing a freshwater injection well or a seawater pumping well in the aquifer, where SWI has progressed [52]. To mitigate SWI damage in advance, seawater pumping at the wedge part of SWI at the bottom [53,54], and conversely, injecting freshwater at the boundary of the SWI area are being researched [55,56]. If intensive response measures are applied to vulnerable areas using the methodology of this study and operational plans are established by considering the vulnerable period, the SWI damage could be effectively reduced, and sustainable utilization of groundwater in the coastal areas could be realized.

Note that this proposed monthly GALDIT method assessed the SWI vulnerability to the relatively large area with sufficient manpower and national monitoring network to detect the temporal variations of groundwater resources. In regions with scarce data or limited infrastructures, the observation period of the data can be selected flexible under efficient data-management plan. For example, long-term historical or future vulnerability can be estimated statistically if data obtained from areas with only recently installed monitoring wells show a constant change per year or show seasonally repeated fluctuation patterns by groundwater exploitation. The applicability of this study could be further expanded if site-specific postprocessing of dynamic parameters, such as moving average.

To employ GALDIT analysis as an assessment tool supporting water-resource management plans, considering vulnerable periods for sustainable operation of coastal groundwater, improving the theoretical weight, and expanding the variable range may be needed

considering static and dynamic parameters representing extreme situations due to climate change in future. Furthermore, a follow-up study is required to improve the equations for calculating GALDIT parameters according to site characteristics.

Author Contributions: Conceptualization, S.W.C. and I.-M.C.; methodology, S.W.C.; validation, I.H.K., S.W.C., and I.-M.C.; investigation, I.H.K.; resources, I.H.K.; data curation, I.H.K.; writing—original draft preparation, I.H.K.; writing—review and editing, S.W.C. and I.-M.C.; visualization, I.H.K.; supervision, I.-M.C.; project administration, S.W.C.; funding acquisition, S.W.C. All authors have read and agreed to the published version of the manuscript.

Funding: This research was supported by a grant from the Development Program of Minimizing of Climate Change Impact Technology funded through the National Research Foundation of Korea (NRF) of the Korean government (Ministry of Science and ICT, Grant No. NRF-2020M3H5A1080735).

Institutional Review Board Statement: Not applicable.

Informed Consent Statement: Not applicable.

Data Availability Statement: Not applicable.

Conflicts of Interest: The authors declare no conflict of interest.

References

- Nicholls, R.J.; Nicholls, P.P.W.; Burkett, V.; Colin, D.W.; Hay, J. Climate change and coastal vulnerability assessment: Scenarios for integrated assessment. *Sustain. Sci.* **2008**, *3*, 89–102. [[CrossRef](#)]
- Howard, K. Urban Groundwater Issues—An Introduction. In *Current Problems of Hydrogeology in Urban Areas, Urban Agglomerates and Industrial Centres*; Springer: Dordrecht, The Netherlands, 2002; pp. 1–15. [[CrossRef](#)]
- Chang, N.-B. *Effects of Urbanization on Groundwater: An Engineering Case-Based Approach for Sustainable Development*; American Society of Civil Engineers: Washington, DC, USA, 2010; ISBN 10:078441078X.
- Chamine, H.I. Water resources meet sustainability: New trends in environmental hydrogeology and groundwater engineering. *Environ. Earth Sci.* **2015**, *73*, 2513–2520. [[CrossRef](#)]
- Bernard-Jannin, L.; Sun, X.; Teissier, S.; Sauvage, S.; Sanchez-Perez, J.M. Spatiotemporal analysis of factors controlling nitrate dynamics and potential denitrification hot spots and hot moments in groundwater of an alluvial floodplain. *Ecol. Eng.* **2017**, *103*, 372–384. [[CrossRef](#)]
- Azimi, S.; Moghaddam, M.A.; Monfared, S.A.H. Spatial assessment of the potential of groundwater quality using fuzzy AHP in GIS. *Arab. J. Geosci.* **2018**, *11*, 142. [[CrossRef](#)]
- Mondal, I.; Bandyopadhyay, J.; Chowdhury, P. A GIS based DRASTIC model for assessing groundwater vulnerability in Jangalmahal area, West Bengal, India. *Sustain. Water Res. Manag.* **2019**, *5*, 557–573. [[CrossRef](#)]
- Ray, S.S.; Ray, A. Major ground water development issues in South Asia: An overview. In *Ground Water Development-Issues and Sustainable Solutions*; Springer: Singapore, 2019; pp. 3–11.
- Custodio, E. Prediction methods, in Hydrology. In *Groundwater Problems in Coastal Areas*; Bruggeman, A.G., Custodio, C., Eds.; Intergovernmental Hydrological Programme, UNESCO: Paris, France, 1987.
- Herzberg, A. Die Wasserversorgung einiger Nordseebäder. *J. Gasbeleucht Wasserversorg* **1901**, *44*, 815–819.
- Ghyben, B.W. Nota in Verband met de Voorgenomen Putboring Nabij Amsterdam. *Tijdschr. K. Inst. Ing.* **1988**, *9*, 8–22.
- Todd, D.K.; Mays, L.W. *Groundwater Hydrology*, 3rd ed.; John Wiley & Sons: New York, NY, USA, 2005.
- Sherif, M.M.; Singh, V.P. Effect of climate change on seawater intrusion in coastal aquifers. *Hydro. Proc.* **1999**, *13*, 1277–1287. [[CrossRef](#)]
- Scanlon, B.; Faunt, C.; Longuevergne, L.; Reedy, R.; Alley, W.; McGuire, V.; McMahon, P. Groundwater depletion and sustainability of irrigation in the US high plains and central valley. *Proc. Nat. Acad. Sci. USA* **2012**, *109*, 9320–9325. [[CrossRef](#)]
- Bobba, A.G. Numerical modelling of salt-water intrusion due to human activities and sea-level change in the Godavari Delta, India. *Hydrol. Sci. J.* **2002**, *47*, S67–S80. [[CrossRef](#)]
- Loáiciga, H.A.; Pingel, T.J.; Garcia, E.S. Seawater intrusion by sea-level rise: Scenarios for the 21st century. *Groundwater* **2012**, *50*, 37–47. [[CrossRef](#)]
- Carretero, S.; Rapaglia, J.; Bokuniewicz, H.; Kruse, E. Impact of sea-level rise on saltwater intrusion length into the coastal aquifer, Partido de La Costa, Argentina. *Cont. Shelf Res.* **2013**, *61–62*, 62–70. [[CrossRef](#)]
- Langevin, C.D.; Zygnerski, M. Effect of sea-level rise on salt water intrusion near a coastal well field in Southeastern Florida. *Groundwater* **2013**, *51*, 781–803. [[CrossRef](#)]
- Rasmussen, P.; Sonnenborg, T.O.; Gonciar, G.; Hinsby, K. Assessing impacts of climate change, sea level rise, and drainage canals on saltwater intrusion to coastal aquifer. *Hydro. Earth Syst. Sci.* **2013**, *17*, 421–443. [[CrossRef](#)]
- Sefelnasr, A.; Sherif, M. Impacts of seawater rise on seawater intrusion in the Nile Delta aquifer, Egypt. *Groundwater* **2014**, *52*, 264–276. [[CrossRef](#)]

21. El-Kadi, A.I.; Tillery, S.; Whittier, R.B.; Hagedorn, B.; Mair, A.; Ha, K.; Koh, G.-W. Assessing sustainability of groundwater resources on Jeju Island, South Korea, under climate change, drought, and increased usage. *Hydrogeol. J.* **2014**, *22*, 625–642. [[CrossRef](#)]
22. Polemio, M.; Walraevens, K. Recent research results on groundwater resources and saltwater intrusion in a changing environment water. *Water* **2019**, *11*, 1118. [[CrossRef](#)]
23. National Research Council. *Ground Water Vulnerability Assessment: Predicting Relative Contamination Potential under Conditions of Uncertainty*; National Academy Press: Washington, DC, USA, 1993; pp. 42–63.
24. Gogu, R.C.; Dassargues, A. Current trends and future challenges in groundwater vulnerability assessment using overlay and index methods. *Environ. Geol.* **2000**, *39*, 549–559. [[CrossRef](#)]
25. Uricchio, V.F.; Giordano, R.; Lopez, N. A fuzzy knowledge-based decision support system for groundwater pollution risk evaluation. *J. Environ. Manag.* **2004**, *73*, 189–197. [[CrossRef](#)] [[PubMed](#)]
26. Babiker, I.S.; Mohamed, M.A.; Hiyama, T.; Kato, K. A GIS-based DRASTIC model for assessing aquifer vulnerability in Kakamigahara Heights, Gifu Prefecture, Central Japan. *Sci. Total Env.* **2005**, *345*, 127–140. [[CrossRef](#)] [[PubMed](#)]
27. Aller, L.; Bennett, T.; Lehr, J.H.; Petty, R.J.; Hackett, G. *DRASTIC: A Standardized System for Evaluating Groundwater Pollution Potential Using Hydrogeologic Settings*; Environmental Protection Agency NWWA/EPA Series EPA-600/2-87-035; National Water Well Association: Dublin, Ireland, 1987.
28. Civita, M. *Le Carte Della Vulnerabilità Degli Acquiferi All'inquinamento: Teoria&Pratica [Aquifer Vulnerability to Pollution Maps: Theory and Practice]*; Pitagora: Bologna, Italy, 1994.
29. Chachadi, G.; Lobo-Ferreira, J.P. Sea water intrusion vulnerability mapping of aquifers using the GALDIT method. *COASTIN Newsl.* **2001**, *4*, 7–9.
30. Kardan Moghaddam, H.; Jafari, F.; Javadi, S. Vulnerability evaluation of a coastal aquifer via GALDIT model and comparison with DRASTIC index using quality parameters. *Hydrol. Sci. J.* **2017**, *62*, 137–146. [[CrossRef](#)]
31. Bordbar, M.; Neshat, A.; Javadi, S. Modification of the GALDIT framework using statistical and entropy models to assess coastal aquifer vulnerability. *Hydrol. Sci. J.* **2019**, *64*, 1117–1128. [[CrossRef](#)]
32. Bordbar, M.; Neshat, A.; Javadi, S.; Pradhan, B.; Aghamohammadi, H. Meta-heuristic algorithms in optimizing GALDIT framework: A comparative study for coastal aquifer vulnerability assessment. *J. Hydrol.* **2020**, *585*, 124768. [[CrossRef](#)]
33. Klassen, J.; Allen, D. Assessing the Risk of Saltwater Intrusion in Coastal Aquifers. *J. Hydrol.* **2017**, *551*, 730–745. [[CrossRef](#)]
34. Luoma, J.; Ruutu, S.; King, A.W.; Tikkanen, H. Time delays, competitive interdependence, and firm performance. *Strateg. Manag. J.* **2017**, *38*, 506–525. [[CrossRef](#)]
35. Hallal, D.; El Amine, M.K.; Zahouani, S.; Benamghar, A.; Haddad, O.; Ammari, A.; Lobo-Ferreira, J. Application of the GALDIT method combined with geostatistics at the Bouteldja aquifer (Algeria). *Environ. Earth Sci.* **2019**, *78*, 22. [[CrossRef](#)]
36. Lee, J.-Y.; Yi, M.-J.; Song, S.-H.; Lee, G.-S. Evaluation of seawater intrusion on the groundwater data obtained from the monitoring network in Korea. *Water Int.* **2008**, *33*, 127–146. [[CrossRef](#)]
37. Shin, J.; Hwang, S. A Borehole-Based Approach for Seawater Intrusion in Heterogeneous Coastal Aquifers, Eastern Part of Jeju Island, Korea. *Water* **2020**, *12*, 609. [[CrossRef](#)]
38. Chang, S.W.; Chung, I.-M.; Kim, M.-G.; Tolera, M.; Koh, G.-W. Application of GALDIT in Assessing the Seawater Intrusion Vulnerability of Jeju Island, South Korea. *Water* **2019**, *11*, 1824. [[CrossRef](#)]
39. Kim, I.-H.; Yang, J.-S. Prioritizing countermeasures for reducing seawater-intrusion area by considering regional characteristics using SEAWAT and a multi-criteria decision-making method. *Hydrol. Proc.* **2018**, *32*, 3741–3757. [[CrossRef](#)]
40. Chun, J.A.; Lim, C.; Kim, D.; Kim, J.S. Assessing impacts of climate change and sea-level rise on seawater intrusion in a coastal aquifer. *Water* **2018**, *10*, 357. [[CrossRef](#)]
41. Kim, K.-Y.; Seong, H.; Kim, T.; Park, K.H.; Woo, N.; Park, Y.S.; Koh, G.W.; Park, W.-B. Tidal effects on variations of fresh-saltwater interface and groundwater flow in a multilayered coastal aquifer on a volcanic island (Jeju Island, Korea). *J. Hydrol.* **2006**, *330*, 525–542. [[CrossRef](#)]
42. Kim, Y.; Yoon, H.; Kim, G.P. Development of a novel method to monitor the temporal change in the location of the freshwater-saltwater interface and time series models for the prediction of the interface. *Environ Earth Sci.* **2016**, *75*, 882. [[CrossRef](#)]
43. Kuan, W.K.; Jin, G.; Xin, P.; Robinson, C.; Gibbes, B.; Li, L. Tidal influence on seawater intrusion in unconfined coastal aquifers. *Water Res. Res.* **2012**, *48*, W02502. [[CrossRef](#)]
44. Recinos, N.; Kallioras, A.; Pliakas, F.-K.; Schüth, C. Application of GALDIT index to assess the intrinsic vulnerability to seawater intrusion of coastal granular aquifers. *Environ. Earth Sci.* **2014**, *73*, 1017–1032. [[CrossRef](#)]
45. Allouche, N.; Maanan, M.; Gontara, M.; Rollo, N.; Jmal, I. A global risk approach to assessing groundwater vulnerability. In *Environmental Modelling and Software*; Elsevier: Amsterdam, The Netherlands, 2017; Volume 88, pp. 168–182.
46. Gundogdu, K.S.; Guney, I. Spatial analyses of groundwater levels using universal kriging. *J. Earth Syst. Sci.* **2007**, *116*, 49–55. [[CrossRef](#)]
47. Sun, Y.; Kang, S.; Li, F.; Zhang, L. Comparison of interpolation methods for depth to groundwater and its temporal and spatial variations in the Minqin oasis of northwest China. *Environ. Model. Soft.* **2009**, *24*, 1163–1170. [[CrossRef](#)]
48. National Groundwater Information Center. Available online: <http://www.gims.go.kr> (accessed on 22 February 2021).
49. National Geographic Information Institute. Available online: <http://www.ngii.go.kr> (accessed on 22 February 2021).
50. Korea Hydrographic and Oceanographic Agency. Available online: <http://www.khoa.go.kr> (accessed on 22 February 2021).

51. Ministry of Oceans and Fisheries. *Coast Condition Survey Report-West Coast*; Ministry of Oceans and Fisheries: Busan, Korea, 2003.
52. Abarca, E.; Vázquez-Suñé, E.; Carrera, J.; Capino, B.; Gámez, D.; Batlle, F. Optimal design of measures to correct seawater intrusion. *Water Res. Res.* **2006**, *42*. [[CrossRef](#)]
53. Sriapai, T.; Walsri, C.; Phueakphum, D.; Fuenkajorn, K. Physical model simulations of seawater intrusion in unconfined aquifer. *Songklanakarin J. Sci. Technol.* **2012**, *34*, 679–687.
54. Pool, M.; Carrera, J. Dynamics of negative hydraulic barriers to prevent seawater intrusion. *Hydrogeol. J.* **2010**, *18*, 95–105. [[CrossRef](#)]
55. Botero-Acosta, A.; Donado, L.D. Laboratory scale simulation of hydraulic barriers to seawater intrusion in confined coastal aquifers considering the effects of stratification. *Proc. Env. Sci.* **2015**, *25*, 36–43. [[CrossRef](#)]
56. Luyun, R.; Momii, K.; Nakagawa, K. Effects of recharge wells and flow barriers on seawater intrusion. *Groundwater* **2011**, *49*, 239–249. [[CrossRef](#)] [[PubMed](#)]